ELSEVIER

Journal of Power Sources 85 (2000) 261–268

JOURNAL OF POWER SOURCES

www.elsevier.com/locate/jpowsour

Thermal and electrochemical studies of carbons for Li-ion batteries 1. Thermal analysis of petroleum and pitch cokes

W. Jiang [a], T. Tran [b], X. Song [a], K. Kinoshita [a,*]

[a] *Environmental Energy Technologies Division, 90-1142, Lawrence Berkeley National Laboratory, Berkeley, CA 94720, USA*
[b] *Department of Chemistry and Materials Science, Lawrence Livermore National Laboratory, Livermore, CA 94550, USA*

Received 17 March 1999; accepted 6 July 1999

Abstract

Thermal analyses involving simultaneous thermal gravimetric analysis (TGA) and differential thermal analysis (DTA) were used to study the air oxidation of petroleum (fluid and needle cokes) and coal-tar pitch cokes. The intent of this study is to understand the relationship between the structure of carbonaceous materials and their thermal oxidation behavior in air (Part 1). A correlation between the thermal oxidative properties of cokes and their electrochemical Li-intercalation performance is discussed in the following paper (Part 2). The carbon samples were heat-treated at temperatures up to 2800°C, and three thermal parameters were determined — ignition temperature (T_i), temperature maximum (T_m) in the DTA curves, and the temperature at which 15% carbon weight loss was attained (T_{15}). The measurements showed trends that are consistent with prior reports that the active sites on the surface and not the total surface area (TSA) are responsible for the thermal behavior of the carbons. Because of the difference in the graphitizability of petroleum and pitch cokes that was obtained by heat treatment, variations in the thermal parameters were observed. Needle cokes are the most easily graphitized and this is reflected in the higher values of the thermal parameters compared to the fluid and pitch cokes.

Keywords: Thermal analysis; Coke; Oxidation; Li-ion batteries

1. Introduction

Carbonaceous materials in a variety of particle morphologies, size and degree of graphitization have been evaluated in Li-ion batteries. In this application, carbon serves as the host substrate for Li ions in the negative electrode [1–5]. The amount of Li^+ ions that are intercalated or inserted into the carbon structure and the reversibility of the intercalation/deintercalation process depend strongly on the carbon morphology. With graphite, the amount of Li^+ ions that are intercalated is equivalent to 372 mA h g^{-1} (LiC_6), whereas much higher capacities are possible in disordered carbons. The irreversible capacity loss associated with the formation of the protective solid–electrolyte interface (SEI) layer varies approximately linearly with the carbon BET surface areas.

The common structure of graphite consists of hexagonal arrays of carbon atoms that are arranged in layer planes (graphite layer planes) stacked in an ABAB... configuration. In this crystallographic structure, the graphite layer planes [(002) spacing] are separated by 3.354 Å. The weak van der Waals bonds between the layer planes permit facile insertion of foreign ions to form intercalated graphite compounds. Carbon structures that contain layer planes separated by distances that are much greater than 3.354 Å are considered amorphous (or disordered) carbon. In amorphous carbon, the hexagonal arrays are not in alignment as they are in graphite, but instead they are rotated with respect to each other so there is no three-dimensional order. This structure is often referred to as a turbostatic structure. As might be expected, the physical properties of carbonaceous materials vary dramatically because of the variable structure that exists.

Two crystallographic parameters that are commonly used to characterize graphitic carbons are L_c and L_a. These parameters describe the crystallite dimension in the *c*-axis direction (perpendicular to the graphite layer planes) and the *a*-axis direction (parallel to the graphite layer planes). X-ray diffraction (XRD) analysis is commonly

* Corresponding author. Tel.: +1-510-486-7389; fax: +1-510-486-4260; E-mail: k_kinoshita@lbl.gov

0378-7753/00/$ - see front matter
PII: S0378-7753(99)00342-0

used to obtain these parameters [6]. Highly graphitized carbons exhibit L_c and L_a that are typically >100 Å, whereas turbostratic carbons have L_c and L_a that are in the range of 20 Å. Consequently, XRD provides a convenient tool to characterize the crystallographic property of carbon.

There are two distinct types of sites on graphite. These are the basal plane sites, which are associated with the carbons forming the surface of the layer planes, and the edge sites, which involve the terminal sites of the basal planes. The basal plane sites are relatively inactive, and edge plane sites are the usual chemical/electrochemical active sites. The concept of active sites for oxidation reactions involving oxygen chemisorption or gasification was clearly demonstrated by Radovic et al. [7], Laine et al. [8] and Coltharp and Hackerman [9]. However, Lang and Magnier [10] reported that the oxidation rate on the edge and basal planes is comparable, although they acknowledged this was contrary to other studies. These studies show that active sites, which are surface sites that are capable of dissociatively chemisorbing oxygen, are present in carbons and they are primarily associated with edge sites or defects on the carbon surface. This observation suggests that the electrochemical and chemical properties of carbonaceous materials should be influenced by the relative fraction of the active sites. It should be possible, then, to derive a better understanding of the relationship between the physical properties, chemical reactivity and electrochemical behavior of carbonaceous materials by investigating their thermal oxidation behavior.

The oxidation rate and ignition temperature (T_i) of carbonaceous materials in air are strongly dependent on parameters such as the surface area and crystallographic structure [11–14]. Thermal analysis of the oxidation behavior of carbon blacks showed a linear relationship between the temperature at which 15% carbon weight loss is attained (T_{15}) and the surface area [11]. High-surface-area carbon blacks exhibit low T_{15} and vice versa. However, the active surface area and not the total surface area (TSA) is the important parameter controlling the oxidation rate of carbons [7]. Therefore, graphitized carbons with a preponderance of basal plane sites are less reactive than disordered carbons that contain a larger fraction of edge or active sites. Radovic et al. [7] suggested that the emergence of the (110) peak at $2\theta = 43^\circ$ in the XRD spectra of carbon is a strong indication of a decrease in the concentration of active sites. The emergence of the (110) peak shows the presence of a more graphitic carbon, which has a larger fraction of basal plane sites and a diminution of edge sites. In the case of high-surface-area carbon blacks, a large fraction of active sites is present on the surface. Welham and Williams [14] used thermal gravimetric analysis (TGA) to investigate air oxidation of ball-milled graphite and active carbons. The ignition temperature decreased after prolonged ball milling, indicating that the disordered carbon that was formed oxidized more quickly, i.e., reduction in crystallinity is associated with an increased reactivity to oxygen. Honda et al. [13] observed by differential thermal analysis (DTA) that the maximum temperature (T_m) in the exotherm during air oxidation was strongly influenced by the $d(002)$ spacing and L_c of the carbon; T_m increased with an increase in L_c and a decrease in the $d(002)$ spacing. For example, T_m of a carbon black (high $d(002)$ spacing, low L_c) was 511°C and that for spectroscopic graphite (low $d(002)$ spacing, high L_c) was 698°C. These trends are consistent with the hypothesis that a decrease in the concentration of edge sites or active sites in carbon results in slower oxidation kinetics and a shift in T_m to higher temperatures.

Various techniques are used to characterize the physicochemical properties of carbonaceous materials, e.g., transmission electron microscopy (TEM), XRD, and Raman spectroscopy. A convenient method to observe the chemical reactivity of carbons is to monitor their oxidation behavior by measuring the weight loss as carbon reacts with oxygen to form gaseous species such as CO and CO_2. In this paper (Part 1), we present the results obtained by TGA and DTA, which are rapid and sensitive techniques to observe the thermal behavior of carbons. The intent of this study is to understand the relationship between the structure of carbonaceous materials, as determined by their thermal oxidation behavior in air, and the electrochemical performance (i.e., reversible and irreversible capacity for Li intercalation); this aspect is discussed in a subsequent paper [15]. As a practical example of the relationship between thermal analysis and electrochemical performance, it should be noted that Nishi et al. [16] claimed in their U.S. Patent that a carbon with T_m at 671°C exhibited a longer cycle life in Li-ion cells than that obtained with a carbon showing T_m at 745°C.

2. Experimental details

Petroleum (fluid and needle coke) and coal-tar pitch cokes obtained from Superior Graphite (Chicago, IL) were used in this study. The physical properties of the as-received cokes are presented in Table 1. The starting materials are produced at a temperature of approximately 1400°C, and the heat-treatment temperatures (HTTs) used in this study are 1800°, 2100°, 2300° and 2800°C. The samples were heat-treated in an inert environment at these elevated temperatures for 2 h in a laboratory-scale graphitizing furnace (Thermal Technology, Santa Rosa, CA). In the case of the needle cokes, they were air-milled either before or after heat treatment to reduce the particle diameter from 45 μm to an average size of 10 μm.

The microstructure of the cokes was examined by XRD, Raman spectroscopy and TEM. The XRD analyses were performed using a diffractometer (Siemens Diffractometer OSP, Model D500, Germany) to determine the $d(002)$ spacing and crystallite dimension, L_c. The value of L_c was

Table 1
Physical properties of as-received cokes
L_c and L_a are the crystallite dimensions perpendicular to the graphite layer planes and parallel to the graphite layer planes, respectively.

Coke	Particle size (μm)	d(002) Spacing (Å)	L_c (Å)	L_a (Å)	BET surface area ($m^2\ g^{-1}$)
Fluid	22	3.470	78	37	6.8
Coal-tar pitch	11	3.489	46	31	11.2
Needle	45	3.442	112	32	0.4

determined from line-broadening measurements of the (002) diffraction peak using the Debye–Scherrer equation:

$$L_c = \frac{0.89\lambda}{(\beta \cos\theta)}, \quad (1)$$

where λ is the wavelength of the X-ray beam, θ is the Bragg angle, and β is the peak width at half-maximum intensity. The crystallite dimension, L_a is obtained by Raman spectroscopy [17], assuming:

$$L_a = \frac{44}{\left(\frac{I_{1372}}{I_{1576}}\right)}, \quad (2)$$

where I_{1372} and I_{1576} are the integrated intensities of the Raman peaks at 1372 cm^{-1} and 1576 cm^{-1}, respectively. The samples were examined by TEM (Topcon-OO2B) operated at 200 kV and a filament current of about 10 μA.

The thermal analysis experiments were conducted using simultaneous TGA/DTA (SDT 2960, TA Instruments, New Castle, DE) to monitor both the weight change (balance sensitivity, 1 μg) and temperature change (ΔT sensitivity, 0.001°C) of the samples. The experimental procedure consisted of two heating cycles. In the first cycle, the sample was heated in flowing nitrogen (99.999% purity, 100 ml min^{-1}) at 10°C min^{-1} to 1200°C, which eliminated any surface oxygen groups that were present. Because the initial cokes were produced at temperatures above 1200°C, this pretreatment step is not expected to change the crystallographic structure of the cokes. After the sample was cooled to room temperature, the gas was switched to air (Air Zero Grade), and a second heating cycle was conducted on the clean carbon. The temperature was increased at 10°C min^{-1} and the coke was oxidized to CO and CO_2 in air (100 ml min^{-1}). Preliminary studies were conducted with different amounts of carbon to insure that the oxidation rate was not diffusion-controlled. A sample weight of 5–10 mg was found to be appropriate in most experiments.

A preliminary study was undertaken to determine the influence of particle size on the thermal parameters. Three samples of graphitized (2800°C) mesocarbon microbeads (MCMB, Osaka Gas) with an average of 6-, 10- and 25-μm diameter was investigated. An attractive feature of these carbons is their nearly spherical structure. These samples have typical crystallographic parameters of d(002) spacing ~ 3.36 Å, L_c ~ 460 Å, and L_a ~ 600 Å after heat treatment at 2800°C [18]. On the other hand, the different cokes used in the present study have different particle sizes and crystallographic parameters.

The parameters, T_i, T_m and T_{15}, were determined from the thermal measurements by the commercial software package that controlled the instrument. The computer program calculated T_i from the derivative dW/dT where W and T are the weight and temperature of the sample, respectively. The temperature at which dW/dT first deviated from zero is designated as T_i. The other parameters, T_m and T_{15}, were determined by the computer software from the DTA and TGA curves, respectively.

A commercial software program (KaleidaGraph, Synergy Software, Reading, PA) was used to analyze and plot the experimental data. Because of the limited data points obtained for the different cokes, no attempt is made to present statistical information. The software program was used to present a linear fit to show the trend of the data, and this is noted in the figure captions.

3. Results and discussion

There is evidence in the literature [19] that heat treatment to graphitize petroleum cokes is strongly influenced by the type of precursor coke. For example, needle cokes show extremely high graphitizability because of the strong preferred parallel orientation of the turbostatic layer structure and the physical shape of the grains. A delayed coke commonly refers to a coke obtained by carbonization of high-boiling hydrocarbon fractions (heavy residues of petroleum or coal processing) using the delayed coking process (i.e., a thermal process that increases the molecular aggregation or association of the raw material to form extended mesophase domains). When coal-tar pitch is heated, mesophase microspherules are formed in the liquid phase at 350°–450°C. These spherules (precursor to MCMBs), which are composed of oriented polycyclic layers in a lamellar structure, grow in size with continued heat-treatment time. A fibrous structure is also formed when the spherules coalesce and grow. Both the composition and the carbonization conditions of the coal-tar affect the type of coke that is obtained. Needle cokes are produced when the pitch is processed under conditions where the molecules are able to orient themselves in a lamellar structure before carbonization and solidification are completed. Fluid cokes consist of spherulitic grains with a

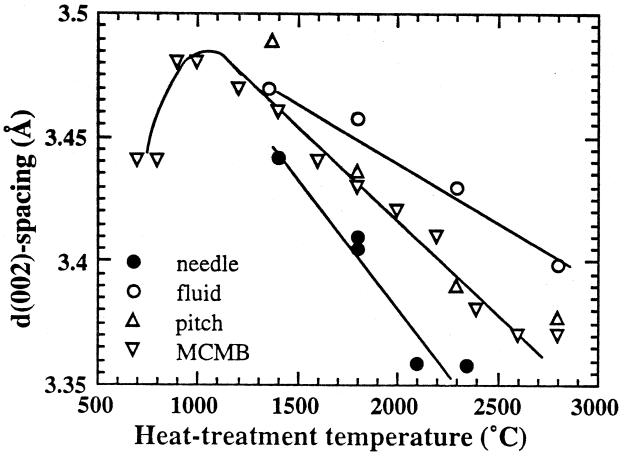

Fig. 1. Change in the $d(002)$ spacing with heat treatment of petroleum and pitch cokes. Line indicates visual trend of the data.

spherical layer structure and they are generally less graphitizable than delayed coke. Furthermore, because of their poor isotropy, they are less suitable for producing isotropic synthetic graphites. Three types of cokes were investigated: (i) fluid coke, (ii) coal-tar pitch delayed coke, and (iii) needle coke; they are referred to as fluid, pitch and needle, respectively, in the figures.

The surface area of particles is inversely proportional to the particle size, assuming that the particles are not porous. Grinding or milling reduces the particle size, and correspondingly, increases the surface area. The cokes used in the present study were subjected to mechanical processing (usually air milling) which has a major influence on the average particle size and surface area. In some samples, the petroleum cokes were air-milled after heat treatment, and the surface areas were considerably higher than those obtained by air milling and then heat treating [20]. The crystallographic parameters, on the other hand, are less sensitive to non-thermal treatment process such as air milling. Consequently, the data obtained for both series of treated cokes are included in this analysis and are useful to understand the relationships between the crystallographic structure parameters (i.e., $d(002)$ spacing, L_c, L_a) of the cokes and their thermal behavior to air oxidation. The variations in particle size complicate the interpretation of the thermal-analysis results obtained from cokes with different particle sizes. Because data on the effect of particle size for cokes were not available, experiments were conducted with MCMBs of average particle sizes between 6 and 25 μm to examine this influence on the thermal parameters.

3.1. Physical property

The influence of heat treatment on the crystallographic parameters, $d(002)$ spacing, L_c and L_a, was clearly evi-

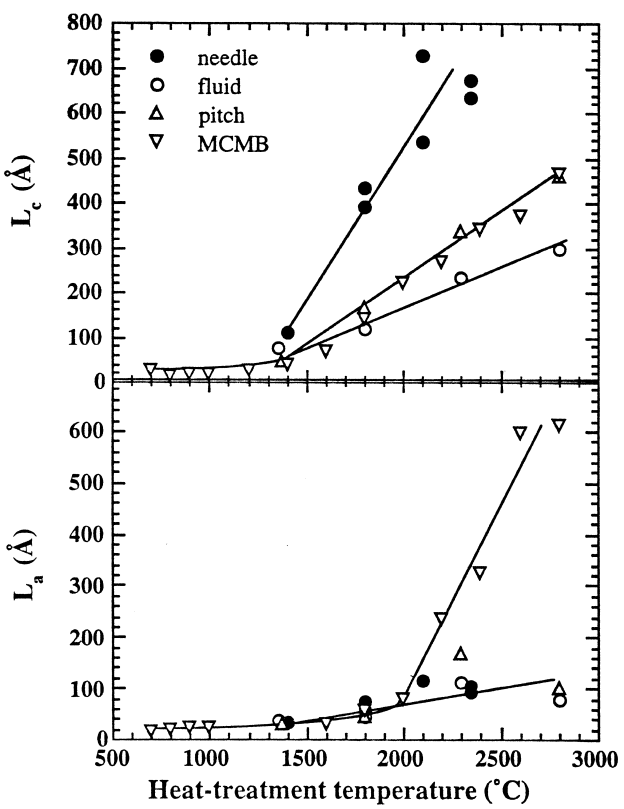

Fig. 2. Change in crystallite parameters, L_c and L_a, of different cokes as a function of HTT. Line indicates visual trend of the data.

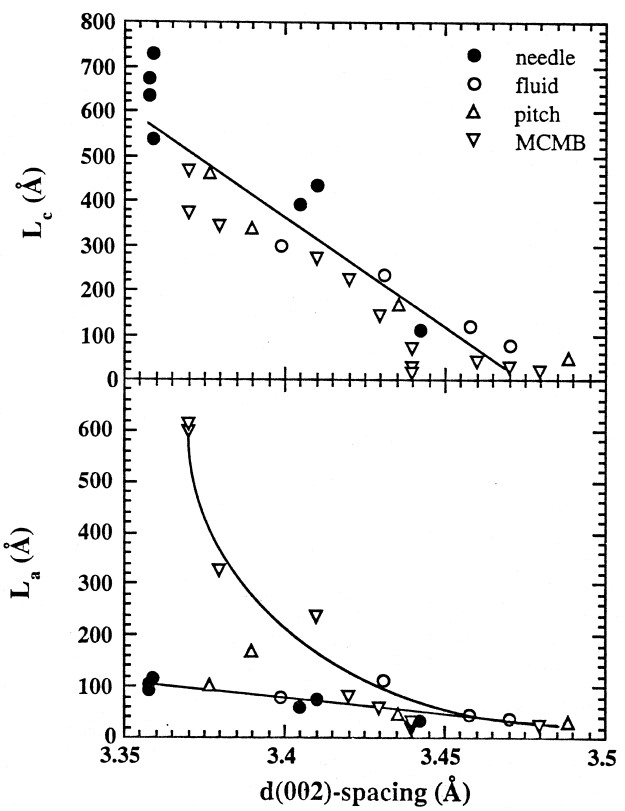

Fig. 3. Plot of $d(002)$ vs. crystallite size of petroleum and pitch cokes. Line indicates visual trend of the data.

dent with the three types of cokes. For comparison purposes, experimental data obtained by Mabuchi et al. [18] with heat-treated MCMBs are included in the figures. The MCMBs are derived from coal-tar pitch, and they represent one of the promising carbons for Li-ion batteries. In the experiments by Mabuchi et al. [18], the MCMBs were heat-treated at temperatures between 700° and 2800°C in an inert environment.

Fig. 1 shows the variations of the carbon interplanar graphene separation, $d(002)$ spacing, as a function of HTTs for various types of cokes and MCMBs. The degree of graphitization, which is commonly correlated to the $d(002)$ spacing, and the rate of graphitization change more rapidly for needle coke than the other two types of cokes. Needle cokes heat-treated at 2350°C for 2 h already showed $d(002)$ spacing approaching close to that of graphite (~ 3.35 Å). It should be noted that the MCMBs and the coal-tar pitch used in the present study showed remarkable similar changes in $d(002)$ spacing with heat treatment at temperatures > 1000°C. The fluid coke appeared to be the least graphitizable, based on the change in $d(002)$ spacing with heat treatment, and this is consistent with published reports [19].

Fig. 2 shows the change in L_c and L_a as a function of heat treatment. These crystallographic parameters increase with an increase in the HTT. The crystallite dimension in

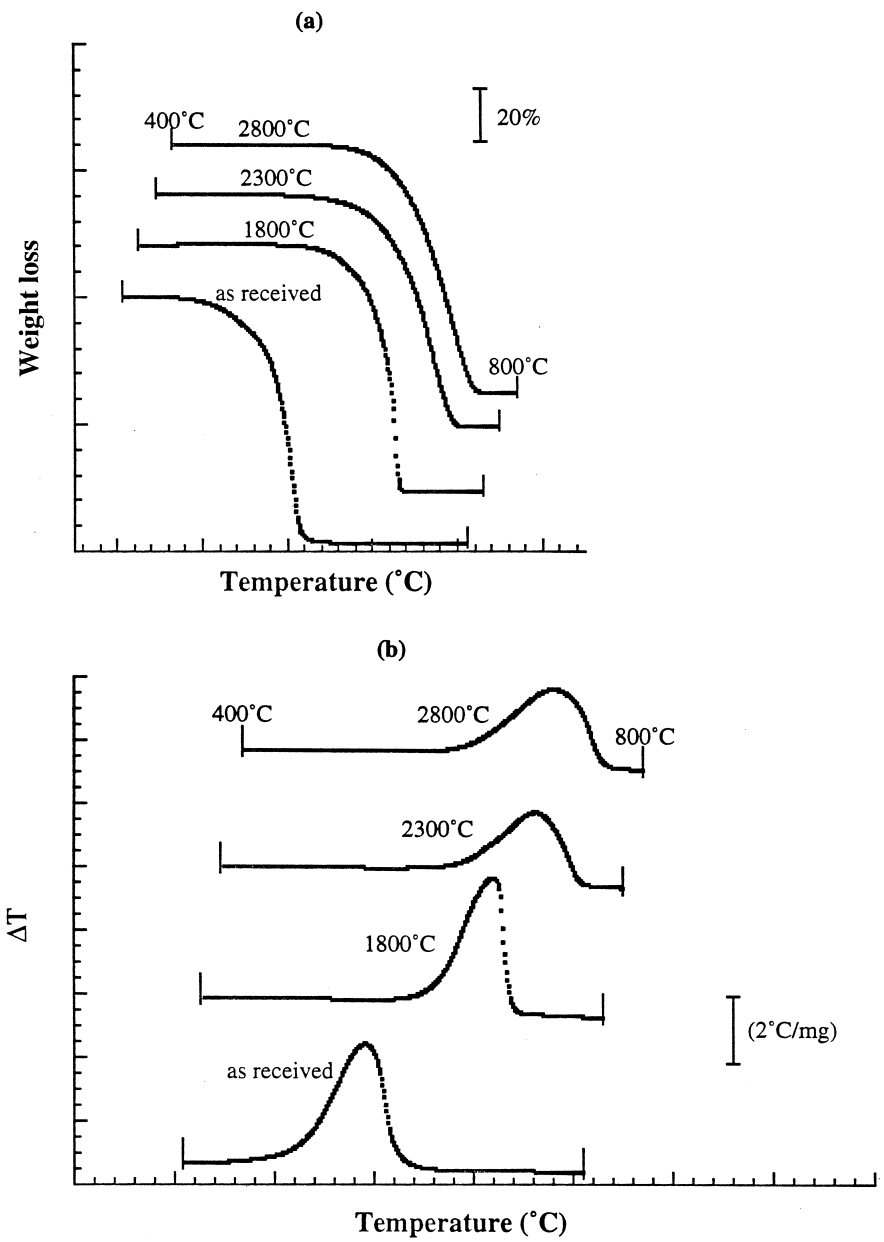

Fig. 4. Typical TGA (a) and DTA (b) traces obtained with pitch coke. Heat rate 10°C min^{-1}. HTTs are indicated. Plots are shifted for clarity to show the traces in the temperature range between 400° and 800°C.

the *c*-axis direction, L_c, for the needle coke increases more rapidly with HTT than that of the MCMB, fluid or coal-tar pitch coke, illustrating the ease of graphitization of needle cokes. Furthermore, the change in L_c of MCMB and pitch cokes with heat treatment is very similar, and increases more rapidly than that for the fluid coke. The increase in L_a with HTT shows no clear indication that the needle coke exhibits a more rapid crystallite growth rate in the *a*-axis direction than that of the other cokes. On the other hand, L_a for the MCMBs increases much more dramatically at temperatures >2000°C compared to the other cokes. A plausible explanation for the divergence in the change of L_a with heat treatment of the MCMBs and the other cokes is not available at this time. However, these results demonstrate that heat treatment is a convenient method to increase the crystallite size, but it is difficult to independently vary the crystallite size in the *c*-axis or *a*-axis direction by this procedure.

The $d(002)$ spacing decreases, and both L_c and L_a increase with an increase in the HTT. These changes in the crystallographic parameters are expected during the carbon-graphitizing process. Fig. 3 shows plots of $d(002)$ vs. L_c and L_a for the different cokes. The trends in the parameters indicate that both L_c and L_a increase with a decrease in the $d(002)$ spacing. It is further noted that L_c increases more rapidly than L_a as the $d(002)$ spacing decreases. With the exception of the MCMBs, the other cokes only exhibit a small change in L_a as the $d(002)$ spacing approaches that of graphite.

3.2. Thermal behavior

Typical examples of the results obtained in the TGA and DTA experiments with pitch coke are presented in Fig. 4a and b, respectively. No perceptible weight change is evident until oxidation begins, which represents the ignition temperature. This is expected because the carbons are initially heated to 1200°C in nitrogen to remove the surface oxides that are present. The TGA curves for the as-received pitch coke and the sample heat-treated at 1800°C show a noticeable difference in the temperature at which rapid oxidation (i.e., steep change in the weight) occurs. On the other hand, only small differences are evident between the weight-loss curves for the pitch cokes that are heat-treated at 2300°C and 2800°C. The ΔT between the carbon sample and alumina reference in the DTA curves diverges significantly when oxidation begins and goes through a maximum (T_m) as oxidation proceeds. Eventually, ΔT decreases as the carbon completely oxidizes.

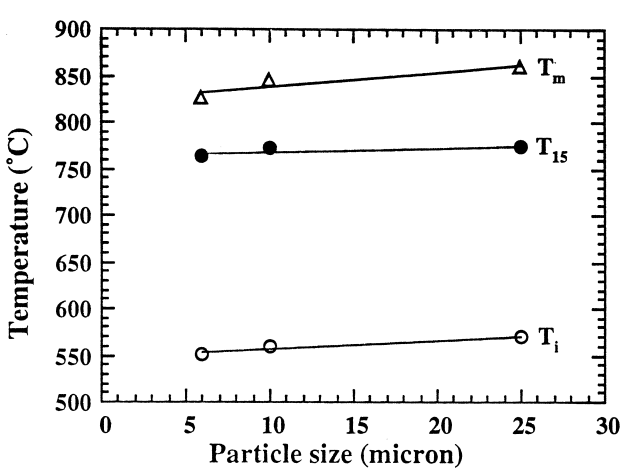

Fig. 5. Variation in thermal parameters, T_i, T_m and T_{15}, of graphitized MCMBs as a function of particle size. Line indicates trend of data from a linear plot using KaleidaGraph.

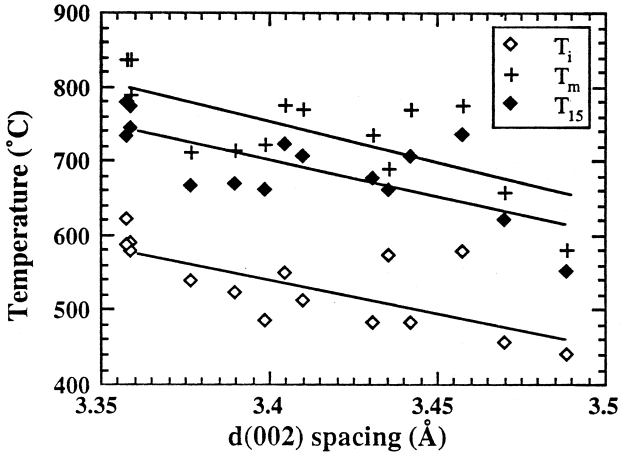

Fig. 6. Composite plot of $d(002)$ spacing and thermal parameters. Line indicates trend of data from linear plot using KaleidaGraph.

The role of particle size on the thermal parameters was investigated using MCMBs because these carbons have a reasonably well-defined spherical structure, and the three samples were heat-treated at the same temperature, 2800°C. The variations in the thermal parameters, T_i, T_m and T_{15}, are plotted in Fig. 5 as a function of particle size. The computer-generated linear plots have slopes of 0.93, 1.59 and 0.46, respectively. They represent an increase of 19°, 34° and 11°C for T_i, T_m and T_{15}, respectively, with increasing particle size in the range between 6 and 25 μm. These results suggest that with nearly spherical particles of graphitized MCMBs, the thermal parameters increase gradually with increasing particle size. Similar studies of the influence of particle size of the coke samples on the thermal parameters were not possible because the particle size was not intentionally varied, while maintaining the crystallographic parameters constant. In fact, the particle size of the different cokes was usually constant and the crystallographic parameters were varied by heat treatment.

The hypothesis presented here is that the thermal parameters are functions of the crystallographic parameters, L_c and L_a. If this is the case, then composite plots of the thermal-analysis data should provide information on the existence of active sites on carbon. The composite plots

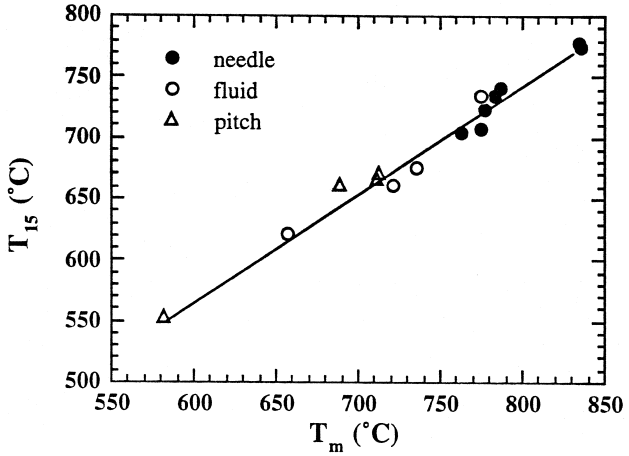

Fig. 7. Relationship between T_m and T_{15} of petroleum and pitch cokes. Line indicates visual trend of the data.

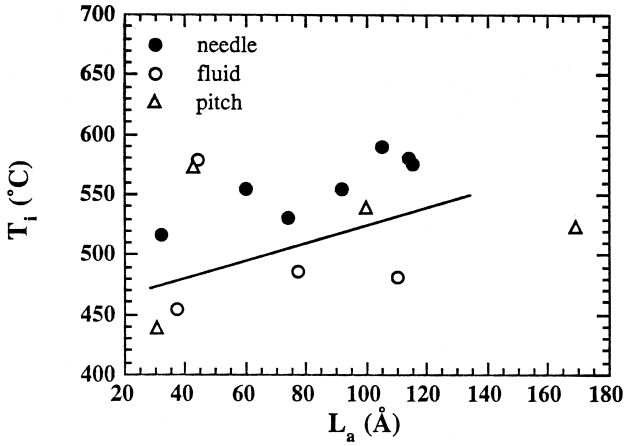

Fig. 9. Relationship between T_i and L_a of petroleum and pitch cokes. Line indicates visual trend of the data.

that are presented in the following figures illustrate the change in thermal behavior that occurs with variations in the crystallographic parameters.

Fig. 6 shows composite plots of the relationship between the $d(002)$ spacing and thermal parameters for the three types of cokes. Despite the scatter in the experimental data, the lines generated by the computer using a software program (KaleidaGraph) illustrate the trends that emerge between the thermal and the degree of graphitization, which is a function of the $d(002)$ spacing for graphitizable carbons. The trend in Fig. 6 indicates that T_i, T_m and T_{15} all increase as the degree of graphitization increases. The temperature maximum (T_m) occurs at a weight-loss in the range 40–60%; therefore, it is considerably higher than that for T_{15}, which corresponds to a weight loss of 15%. This trend is consistent with the concept that more highly graphitized carbons (i.e., lower $d(002)$-spacing) are more difficult to oxidize; hence, higher T_i, T_m and T_{15} are obtained. The data plotted in Fig. 7 clearly show a linear relationship between T_m and T_{15}, and the trend appears to be the same for the three types of cokes. This result indicates that the structural differences between the three types of cokes do not appear to change the linear relationship of T_m and T_{15}, i.e., the proportionality constant is the same for the different cokes used in this study. Although the data are not presented here, both T_m and T_{15} also increase with an increase in T_i.

The results presented in Fig. 6 show the general trends that are observed between the thermal parameters and the three types of cokes. However, no clear distinction is evident in Fig. 6 to indicate the differences in the thermal parameters between the three types of cokes. In the following figures (Figs. 8–10), the data are plotted to delineate the differences that may be present. Fig. 8 shows a plot of T_i and the HTT of the three types of cokes. With the exception of the data points at 1800°C for the fluid and pitch cokes, it appears that T_i for the needle coke occurs at a higher temperature than that for the other two types of carbons. Because of the ease of graphitization of the needle coke, it has a higher degree of graphitization at a given HTT (see Fig. 1, the degree of graphitization is inversely related to the $d(002)$ spacing) than the other two

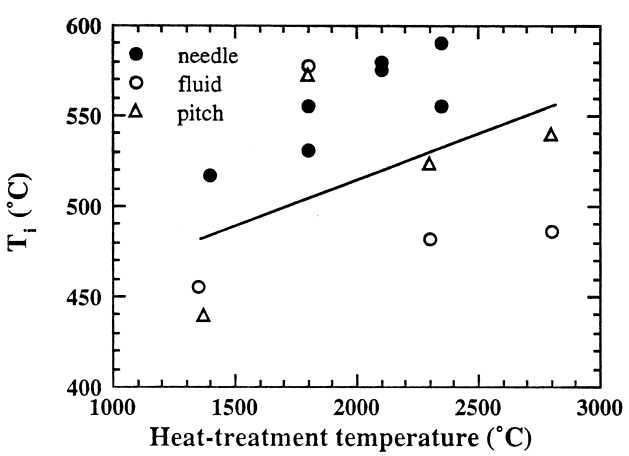

Fig. 8. Relationship between T_i and HTT of petroleum and pitch cokes. Line indicates visual trend of the data.

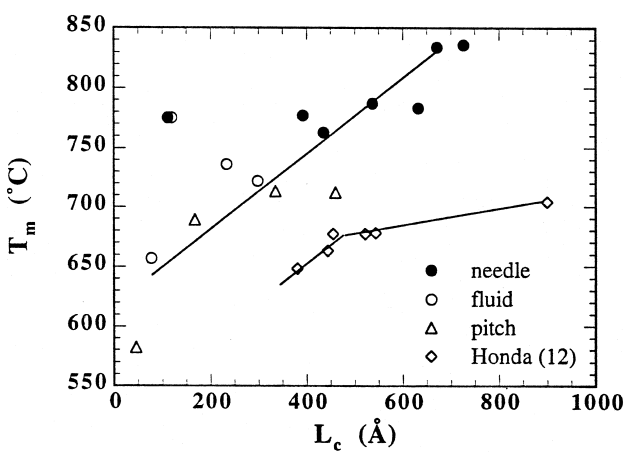

Fig. 10. Relationship between T_m and L_c. Results from this study and Honda et al. [13]. Line indicates visual trend of the data.

cokes. Consequently, the needle coke has a higher T_i at a given HTT than the other cokes. When the relationship between T_i and L_a (see Fig. 9) and T_i and L_c (see Fig. 10) are plotted, the results suggest a similar trend to that observed in Fig. 8, i.e., the needle coke has a higher T_i at a given value of L_a or L_c than that of the fluid and pitch cokes. An analysis of the relationship between T_i and $d(002)$ spacing (results not plotted here) also showed a similar but weak trend. These results suggest that the crystallographic parameters of coke influence the ignition temperature.

Honda et al. [13] conducted TGA/DTA studies on the oxidation of reactor-grade graphite and presented results on the variation of T_m with L_c. Their DTA studies showed that T_m decreased with a decrease in the $d(002)$ spacing and an increase in L_c. However, their measurements were limited to a narrow range of $d(002)$ spacings, i.e., about 3.35 to 3.37 Å, and L_c represented the upper range of crystallite sizes (about 400–1000 Å) used in our studies. Their results are included in the data in Fig. 10 from the present study. It is evident that the results from Honda et al. and the three types of cokes show a similar trend indicative of an increase in T_m (for T_m less than about 500°C) with an increase in L_c. However, our results show that a higher T_m is observed with the cokes. For T_m greater than about 500°C, the results from Honda et al. [13] show a marked divergence. At this time, the difference between the results is unclear and may be an artifact from differences in the way the experiments were conducted.

In summary, analysis of the thermal parameters and the crystallographic structure of the three types of cokes show that T_i, T_m and T_{15} increase with an increase in L_c and L_a and a decrease in the $d(002)$ spacing. These results are consistent with the presence of a higher fraction of active surface sites in less-graphitic carbons that are susceptible to oxidation at lower temperatures. When the cokes are heat-treated at higher temperatures, a more graphitic structure is formed that is resistant to oxidation, and consequently T_i, T_m and T_{15} shift to higher temperatures.

4. Concluding remarks

Simultaneous TGA/DTA measurements were made to investigate the thermal parameters of cokes during air oxidation. The temperatures T_i, T_m and T_{15} are derived from the thermal-analysis measurements, and they are influenced by the crystallographic parameters of the cokes. Definite trends were evident between the thermal parameters and the crystallographic parameters of the different cokes used in the study.

Radovic et al. [7] suggested that the relative fraction of active sites on the carbon surface is a function of L_a; an increase in L_a is associated with a decrease in the fraction of active sites. If the oxidation behavior of carbons, as determined by T_i, T_m and T_{15}, is controlled by the presence of active sites, then a correlation between L_a and the thermal parameters should be evident. The results of the present study support this contention, and the earlier conclusions by Radovic et al. [7], Laine et al. [8] and Coltharp and Hackermann [9] that the active sites are important factors controlling the oxidation of cokes.

Acknowledgements

This work was supported by the Assistant Secretary for Energy Efficiency and Renewable Energy, Office of Advanced Automotive Technologies of the U.S. Department of Energy under Contract No. DE-AC03-76SF00098 at Lawrence Berkeley National Laboratory and Contract No. W-7405-ENG-48 at Lawrence Livermore National Laboratory. The authors would like to acknowledge Superior Graphite and Osaka Gas for kindly supplying the carbon samples used in this study.

References

[1] K. Kinoshita, Advanced anode materials for Li-ion batteries, in: T. Osaka, M. Datta (Eds.), New Trends in Electrochemical Technology: Energy Storage Systems for Electronics, Gordon and Breach Science Publishers, Reading UK, 1999, to be published.
[2] J. Besenhard, M. Winter, in: Tagungsband, W. Schmickler (Eds.), Ladungsspeicherung Doppleschicht, Ulmer Elektrochem. Tage, 2nd, 1994, Universitaetsverlag, Ulm., Germany, 1995, p. 47.
[3] J. Tarascon, D. Guyomard, Electrochim. Acta 38 (1993) 1221.
[4] D. Guyomard, J. Tarascon, Solid State Ionics 69 (1994) 222.
[5] S. Hossain, in: D. Linden (Ed.), Handbook of Batteries, 2nd edn., McGraw-Hill, New York, 1995, p. 36.1.
[6] F. Feret, Analyst 123 (1998) 595.
[7] L. Radovic, P. Walker, R. Jenkins, Fuel 62 (1983) 849.
[8] N. Laine, F. Vastola, P. Walker, J. Phys. Chem. 67 (1963) 2030.
[9] M. Coltharp, N. Hackerman, J. Phys. Chem. 72 (1968) 1171.
[10] F. Lang, P. Magnier, Chem. Phys. Carbon 3 (1968) 121.
[11] E. Charsley, J. Dunn, Rubber Chem. Technol. 55 (1982) 382.
[12] A. Kirshenbaum, Thermochim. Acta 18 (1977) 113.
[13] T. Honda, T. Saito, Y. Horiguchi, Tanso 72 (1972) 14.
[14] N. Welham, J. Williams, Carbon 36 (1998) 1309.
[15] T. Tran, B. Yebka, X. Song, G. Nazri, K. Kinoshita, D. Curtis, J. Power Sources, Part 2, submitted.
[16] Y. Nishi, H. Azuma, A. Omaru, Sony, U.S. Patent 4,959,281, Sept. 25, 1990.
[17] F. Tuinstra, J. Koenig, J. Chem. Phys. 53 (1970) 1126.
[18] A. Mabuchi, K. Tokumitsu, H. Fujimoto, T. Kasuh, J. Electrochem. Soc. 142 (1995) 1041.
[19] H. Marsh, E. Heintz, F. Rodriguez-Reinoso (Eds.), Introduction to Carbon Technologies, University of Alicante, Spain, 1997.
[20] T. Tran, L. Spellman, W. Goldberger, X. Song, K. Kinoshita, J. Power Sources 68 (1997) 106.